

# Carbonization of Highly Oriented Poly(tetrafluoroethylene)

Ladislav Kavan,\* František P. Dousek, Pavel Janda, and Jan Weber

*J. Heyrovský Institute of Physical Chemistry, Dolejškova 3, 182 23 Prague 8, Czech Republic*

*Received August 10, 1998. Revised Manuscript Received November 12, 1998*

Defluorination of a film of highly oriented poly(tetrafluoroethylene) (PTFE) was carried out by the action of lithium and sodium amalgams. The reaction yields a composite product containing carbon with the equivalent amount of alkali metal fluoride. This material was studied by X-ray photoelectron spectroscopy, Raman spectroscopy, and atomic force microscopy. The carbonized film is sensitive to surface oxidation upon contact to air. Part of the carbon in the product shows an unusual structure based on sp-bonded carbon chains. The amalgam-induced defluorination of PTFE influences markedly the surface morphology on the micron scale. Moreover, the molecular-level ordering of the precursor is reconstructed in the product of carbonization, presumably due to oxidative breakdown.

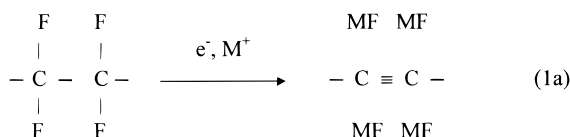
## 1. Introduction

Carbonization of poly(tetrafluoroethylene) (PTFE) and other perhalogenated hydrocarbons can be carried out at room temperature by strong reductants or electrochemically.<sup>1,2</sup> The electrochemical dehalogenation proceeds either on a metal cathode in aprotic electrolyte solutions or, to advantage, in a cell with an alkali metal (M = Li, Na, K) amalgam anode. The latter is formed spontaneously at the PTFE/amalgam interface:<sup>3</sup>



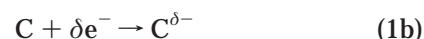
The thermodynamic cell voltage equals 3.251 V for M = Li at 25 °C. C–MF denotes the reaction product, i.e., a conducting (e<sup>-</sup>/M<sup>+</sup>) mixture of carbon with the alkali metal fluoride.<sup>1,2</sup>

Carbon in the C–MF composite shows unique electrical and optical properties (for a review, see ref 2). They were correlated with a model structure of sp-bonded carbon chains (polyynes), formed during the cathodic defluorination of PTFE:



The presence of polyynes in the product of reaction 1a is supported, for example, by a strong Raman line at 2000 cm<sup>-1</sup>.<sup>4,5</sup> Strictly speaking, this assignment is not unambiguous, since identical features can be expected also for polycumulene (polyallene), =(C=C)<sub>n</sub>.<sup>4,6</sup> The

only argument in favor of the alternating polyyne structure is its theoretically higher stability because of Peierls distortion. The defluorination (eq 1a) is inherently accompanied by a small over-reduction, i.e., n-doping of the formed elemental carbon:



The doping level,  $\delta$ , equals 0.2 e<sup>-</sup>/C-atom, independent of the alkali metal type, M.<sup>2,7</sup>

Electrochemical carbonization of oriented PTFE is expected to be anisotropic with preferential carbonization along the aligned PTFE chains. This was first demonstrated on the ram-extruded PTFE rod<sup>8,9</sup> and stretch-oriented PTFE foils (ref 1, p 86). Raman spectra of C–NaF from stretch-oriented PTFE foil indicate the presence of partly oriented polyyne chains with an average conjugation length of 16 carbon atoms (eight conjugated triple bonds) in the direction of alignment.<sup>5</sup>

Application of atomic force microscopy (AFM) technique for high-resolution imaging requires surfaces with low corrugation, close to the size of the structures studied. Thus, for molecular imaging, the preparation of an atomically flat surface (preferably with ordered structure) is of high importance. The friction-deposition of PTFE films allows preparation of highly oriented PTFE chains<sup>10</sup> in the form of thin layers on glass,<sup>10–13</sup> Pt,<sup>14,15</sup> Si,<sup>15–17</sup> diamond-like carbon,<sup>18</sup> Au, graphite (HOPG), and TiN.<sup>14</sup>

Schott<sup>17</sup> has reported that such PTFE films are reducible via the vacuum deposition of sodium metal.

(1) Kavan, L. In *Chemistry and Physics of Carbon*, Vol. 23; Throrer, P. A., Ed.; Marcel Dekker: New York, 1991; pp 69–171.

(2) Kavan, L. *Chem. Rev.* **1997**, *97*, 3061.

(3) Jansta, J.; Dousek, F. P.; Riha, J. *J. Appl. Polym. Sci.* **1975**, *19*, 3201.

(4) Kastner, J.; Kuzmany, H.; Kavan, L.; Dousek, F. P.; Kürti, J. *Macromolecules* **1995**, *28*, 344.

(5) Kavan, L.; Hlavaty, J.; Kastner, J.; Kuzmany, H. *Carbon* **1995**, *33*, 1321.

(6) Kürti, J.; Magyar, C.; Balazs, A.; Rajczy, P. *Synth. Met.* **1995**, *71*, 1865.

(7) Kavan, L.; Dousek, F. P.; Micka, K. *Solid State Ionics* **1990**, *38*, 109.

(8) Barker, D. J.; Brewis, D. M.; Dahm, R. H.; Hoy, L. R. J. *J. Mater. Sci.* **1979**, *14*, 749.

(9) Dahm, R. H.; Barker, D. J.; Brewis, D. M.; Hoy, L. R. J. In *Adhesion 4*; Allen, K. W., Ed.; Applied Science Publ: London, 1980; pp 215–232.

(10) Wittmann, J. C.; Smith, P. *Nature* **1991**, *352*, 414.

(11) Fenwick, D.; Ihn, K. J.; Motamedi, F.; Wittmann, J. C.; Smith, P. *J. Appl. Polym. Sci.* **1993**, *50*, 1151.

However, the carbonization was not complete: XPS indicated the surface stoichiometry only between CF and C<sub>2</sub>F.<sup>17</sup>

This paper scrutinizes the salient features of electrochemical reductive carbonization of friction-deposited PTFE films.

## 2. Experimental Section

PTFE films were prepared from commercial-grade foils (Goodfellow UK, 1 mm thick) by friction deposition (hot-dragging method)<sup>10</sup> on three different supports: Si wafers (OKMETIC Finland), ordinary microscope glass, and rock-salt single crystals (cut to ca. 10 × 10 × 5 mm). Angle-resolved XPS indicated that the Si wafers contained a surface oxidic layer of the thickness of about 5 nm. The film was deposited from the as-received (nonbeveled) PTFE; the substrate temperature was 270 °C (measured with contact thermocouple), the load 2–5 N, and the speed 0.6 mm/s. For further preparative details, see refs 10 and 19. After deposition, the samples were allowed to cool freely to room temperature. The Si- and NaCl-supported films were tested by FTIR transmission spectroscopy, while it was found that the intensity of the characteristic IR bands of PTFE did not change dramatically when varying the load and speed during the film preparation. Typical optical density of NaCl/PTFE film was 0.04 at 1152 cm<sup>-1</sup> (ν C–F). Assuming that the Beer law is valid, this would translate into an effective PTFE thickness of about 100 nm. Under comparable conditions, the Si/PTFE films were mostly thinner; their estimated thickness was about 20–50 nm. These values also match the typical maximum surface corrugation observed by AFM.

Lithium (from BDH, containing 0.7 wt % Na and 0.01 wt % K) and sodium (from BDH, containing 5 × 10<sup>-4</sup> wt % Li) were dissolved in polarographic grade mercury (99.9999%, Sluzba výzkumu, CR) to a concentration of 0.9–1.2 atom %. Details on the amalgam preparation, purification, and chemical analysis are described elsewhere.<sup>7</sup> During the experiments, **care should be taken** because the dissolution of alkali metal (especially Na) in mercury is highly exothermic, which may cause uncontrolled overheating of the mixture. To avoid these hazards, the alkali metal must be added only slowly in small pieces and with good cooling.

The PTFE films were outgassed at 100 °C/1 mPa and subsequently contacted at room temperature with the amalgam. After about 1 h of reaction, the carbonized film was washed with pure mercury. All operations were carried out under high vacuum in sealed all-glass apparatus. In some cases, this apparatus was vacuum-connected to a quartz optical cell (Helma 220 QS, 1 × 1 cm), which served for in situ Raman measurements (see ref 4 for experimental details). For comparison, also carbonized layers (C–MF, thickness about 1 μm) were prepared on ordinary (nonoriented) PTFE foil (0.1 mm, from ICI).

Atomic force microscopy studies were carried out on scanning probe microscope TMX 2010 Discoverer (TopoMetrix), with a pyramidal Si<sub>3</sub>N<sub>4</sub> AFM tip (1520 Standard, TopoMetrix). All measurements were made at the ambient atmosphere and temperature. Static charge formation and accumulation on the

sample surface during AFM scanning was prevented by an ionizer <sup>241</sup>Am (α, 50 MBq).

X-ray photoelectron spectra (XPS) were measured on a VG Scientific ESCA 3 Mk II electron spectrometer with the pressure of residual gases lower than 0.1 μPa. Spectra were excited by Al Kα radiation (hν = 1486.6 eV). The hemispherical electron analyzer was operated in the fixed transmission mode with a band-pass energy of 20 eV, giving the width of 1.1 eV for the Au 4f<sub>7/2</sub> spectral line. Static sample charging was corrected by assigning the value of 284.8 eV to the CH<sub>x</sub> (C 1s) peak from the hydrocarbon impurity. The peak area was calculated after removal of the satellite lines Kα<sub>34</sub> and nonlinear background.<sup>20</sup> The overlapping spectral features were resolved into individual components by using a modified procedure of Hughes and Sexton.<sup>21</sup> The curve-fitting program used the computer-optimized positions of the peaks with constant fwhm values. Depending on the sample, the fwhms were in the range of 1.7–1.9 eV (C1s), 2.0–2.4 eV (F1s), and 2.8–3.0 eV (O1s). The surface concentrations were determined by using the Scofield's subshell photoionization cross section<sup>22</sup> corrected for the attenuation electron lengths.<sup>23</sup> The samples were installed into the spectrometer after a short contact (minutes) to air.

Raman spectra were measured in situ using a high-resolution XY multichannel Raman spectrometer T64000 (Jobin/Yvon, France) equipped by a liquid N<sub>2</sub> cooled (140 K) low noise CCD detector. The samples were positioned in evacuated quartz optical cells (see above). The spectra were excited in a 180° backscattering geometry by Ar<sup>+</sup> laser (Innova 305, Coherent, USA), λ = 488 nm. The laser power was set to 1.5–2.0 mW. Under these conditions, the Raman spectra did not change markedly during repeated data collection, which indicated no significant photodecomposition effects. The spectral resolution was 23 cm<sup>-1</sup>, and the total accumulation time about 1 h.

## 3. Results and Discussion

**3.1. XPS Spectra.** Figure 1 shows XPS spectra in the C1s and F1s regions of the glass-supported PTFE films before (Figure 1a) and after (Figure 1b) the treatment with Li amalgam. The spectra of PTFE and C–MF (M = Li, Na) on glass, Si, and NaCl exhibited qualitatively similar features. The binding energies and surface concentrations for the PTFE–Li amalgam system are summarized in Table 1. Besides the given elements (and SiO<sub>x</sub> from the support), also Li and trace amounts of Na were detected in C–LiF films. Values for Li were, however, poorly reproducible due to low photoionization cross section of Li1s.

A sole XPS measurement of poly(tetrafluoroethylene) is not a trivial problem, because of X-ray-induced cross-linking.<sup>24</sup> The F1s level is not very sensitive to this effect, but there appear several new low-binding-energy C1s peaks assigned to CF<sub>x</sub> (x = 0–3) species. Since this occurs already at very low X-ray doses, doubts exist whether it is even possible to obtain any XPS spectrum of PTFE free of radiation damage.<sup>24</sup> Our data (Figure 1, Table 1, PTFE peaks C<sup>β</sup>, C<sup>γ</sup>) seem to show also weak cross-linking. Studies of oriented PTFE films have been more concentrated at the UPS studies of the valence band,<sup>15,17</sup> where the sample decomposition is, presumably, less significant. The X-ray induced cross-linking

(12) Hansma, H.; Motamedi, F.; Smith, P.; Hansma, P. *Polymer* **1992**, *33*, 647.

(13) Dietz, P.; Hansma, P. K.; Ihn, K. J.; Motamedi, F.; Smith, P. *J. Mater. Sci.* **1993**, *28*, 1372.

(14) Bodo, P.; Ziegler, C.; Rasmussen, J. R.; Salaneck, W. R.; Clark, D. T. *Synth. Met.* **1993**, *55–57*, 329.

(15) Fahlman, M.; Clark, D. T.; Beamson, G.; Fredriksson, C.; Salaneck, W. R.; Logdlund, M.; Lazzaroni, R.; Bredas, J. L. *Synth. Met.* **1993**, *55–57*, 74.

(16) Fahlman, M.; Rasmussen, J.; Kaeriyama, K.; Clark, D. T.; Beamson, G.; Salaneck, W. R. *Synth. Met.* **1994**, *66*, 123.

(17) Schott, M. *Synth. Met.* **1994**, *67*, 55.

(18) Yang, E.; Hirvonen, J. P. *Thin Solid Films* **1993**, *226*, 224.

(19) Beamson, G.; Clark, D. T.; Deegan, D. E.; Hayes, N. W.; Law, D. S. L.; Rasmussen, J. *Surf. Interface Anal.* **1996**, *24*, 204.

(20) Shirley, D. A. *Phys. Rev. B* **1972**, *5*, 4709.

(21) Hughes, A. E.; Sexton, B. A. *J. Electron Spectrosc. Relat. Phenom.* **1988**, *46*, 31.

(22) Scofield, J. H. *J. Electron Spectrosc. Relat. Phenom.* **1976**, *8*, 129.

(23) Seah, M. P.; Dench, W. A. *Surf. Interface Anal.* **1979**, *1*, 2.

(24) Rye, R. *J. Polym. Sci. B: Polym. Phys.* **1993**, *31*, 357.

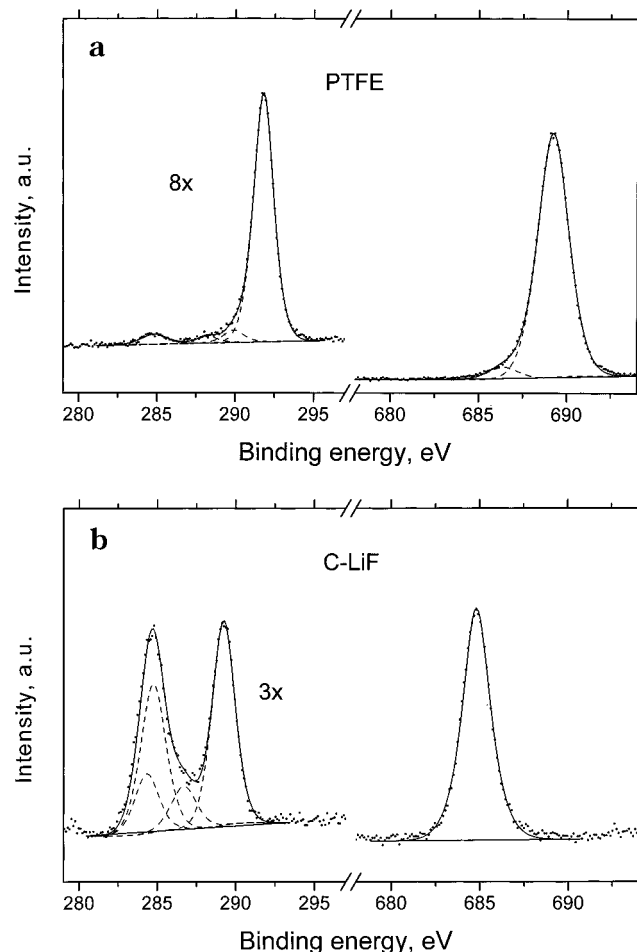


**Figure 1.** (a) XPS spectra (C1s, F1s) of the oriented PTFE film deposited on glass. Note the different intensity scales. (b) XPS spectra (C1s, F1s) of the C-LiF film deposited on glass. The sample was prepared from oriented PTFE (Figure 1a) via treatment with Li amalgam at 25 °C. Note the different intensity scales.

**Table 1. Results of XPS Analysis of PTFE Films<sup>a</sup>**

		C1s		F1s		O1s O/C <sup>α</sup>
		C	E <sub>b</sub> (eV)	C/C <sup>α</sup>	E <sub>b</sub> (eV)	
glass/PTFE virgin	C <sup>α</sup>	284.8	1.00	689.2	51.9	2.60
	C <sup>β</sup>	288.2	0.63	686.5	2.31	
	C <sup>γ</sup>	289.9	1.14			
	C <sup>δ</sup>	291.8	22.9			
glass/PTFE carbonized	C <sup>α</sup>	284.6	1.00	684.8	0.58	3.24
	C <sup>β</sup>	284.8	2.57			
	C <sup>γ</sup>	286.7	0.79			
[C-LiF] Si/PTFE virgin	C <sup>δ</sup>	289.4	3.50			0.10
	C <sup>α</sup>	284.8	1.00	689.5	6.30	
	C <sup>β</sup>	285.2	0.98			
	C <sup>γ</sup>	288.5	0.20			
Si/PTFE carbonized	C <sup>δ</sup>	292.5	2.95			3.87
	C <sup>α</sup>	284.6	1.00	684.6	1.03	
	C <sup>β</sup>	284.8	2.14			
	C <sup>γ</sup>	286.5	0.29			
[C-LiF]	C <sup>δ</sup>	288.5	0.43			

<sup>a</sup> Binding energies and surface concentrations are given for the samples before and after the treatment with Li amalgam (cf. Figure 1).

of oriented and ordinary PTFE might be interestingly different, but a deeper study is beyond the scope of this paper. Our binding energies of Si/PTFE (Table 1) agree well with those observed by other authors<sup>19</sup> for the same system (292.60 and 689.85 eV).

The XPS spectra of PTFE treated by Li or Na amalgams display a complete disappearance of the fluoropolymer C1s (292 eV) and F1s (689 eV) peaks. Hence, the fluoropolymer has been quantitatively converted (at least within the probing depth of the XPS analysis, ≈4 nm) into the carbon-alkali metal fluoride composite (C-MF). [However, the actual carbonization depth is larger, since no PTFE-related features appear also in the Raman spectra (see section 3.3).] The quantitative defluorination of oriented PTFE film resembles the same reaction of "ordinary" PTFE with alkali metal amalgams,<sup>1,2,25</sup> but it contrasts with the reactivity of both oriented<sup>17</sup> and ordinary<sup>26</sup> PTFE with pure alkali metals (sodium vapor). In the later case, poorly defined products of a surface composition of CF<sub>x</sub> (0 < x < 3) resulted. Badyal et al.<sup>26</sup> have fitted the C1s spectra of Na-treated PTFE to six components: -C<sub>x</sub>- (284.3 eV), CCF<sub>n</sub> (286.6 eV), =CFC (288.3 eV), =CCF<sub>n</sub>- (289.5 eV), -CF<sub>2</sub>- (291.2 eV) and -CF<sub>3</sub>- (293.6 eV). A complete defluorination was not achieved, even after prolonged exposure to sodium vapor, which leads eventually to a surface metalization. The mechanism of Na-induced defluorination was not elucidated because of its complexity.<sup>26</sup>

We have suggested an interpretation that PTFE reacts with gaseous or liquid alkali metals (also with highly concentrated Na amalgam at 100 °C) via uncontrolled permeation of the reactants through cracks in the partly carbonized layer.<sup>7</sup> On the other hand, the defluorination of PTFE with diluted alkali metal amalgams at room-temperature proceeds "indirectly" via a charge (e<sup>-</sup>/M<sup>+</sup>) transport through C-MF. This process sets in after a short initialization period, when the primary interfacial layer is formed by a "direct" chemical contact of the reactants. The subsequent "indirect" propagation of the reaction is described by an electrochemical model.<sup>1-3</sup> The amalgam-induced carbonization of PTFE (and other perfluorinated polymers) is characterized by quantitative defluorination and well-defined kinetics. The latter is described by the equation<sup>2,3,27</sup>

$$L = L_0 + kt^{1/2} \quad (2)$$

where  $L$  is the thickness of the carbonized PTFE layer during the reaction time,  $t$ , and  $L_0$  is the thickness of the primary layer. The rate constant,  $k$ , equals (in nm s<sup>-1/2</sup> and at 25 °C) 47.5 (for Li) and 2.67 (for Na).<sup>7</sup> The primary layer ( $L_0$ ) is formed in C-NaF [from poly-(tetrafluoro-*co*-hexafluoropropene)] during <1 min and its thickness,  $L_0$ , is on the order of 10<sup>1</sup> nm.<sup>27</sup> There are no corresponding data for C-LiF, because this system is too fast to be studied by the same methods as C-NaF.<sup>27</sup> (The primary layer is negligible in experiments with PTFE foils, where the  $L$  values are typically in the micrometer to millimeter domain<sup>2</sup>).

According to eq 2, the 100 nm thick film of PTFE would theoretically be converted into C-LiF or C-NaF in <4 s or <23 min, respectively. (Carbonization times are smaller than the given values, because  $L_0$  cannot

(25) Kavan, L.; Bastl, Z.; Dousek, F. P.; Jansta, J. *Carbon* **1984**, *22*, 77.

(26) Tasker, S.; Chambers, R. D.; Badyal, J. P. S. *J. Phys. Chem.* **1994**, *98*, 12442.

(27) Kavan, L.; Micka, K.; Kastner, J. *Synth. Met.* **1994**, *63*, 147.

be neglected at the layer thickness of 100 nm). The carbonization rate of oriented PTFE is unknown, except for a qualitative conclusion that it is anisotropic, i.e., faster in the direction along the oriented chains.<sup>8,9</sup> The oriented PTFE films are interesting systems in which to study the primary ("chemical") contact of PTFE and amalgam. Our analyses clearly evidence that the primary, short-range chemical reaction leads to a quantitative defluorination, like the subsequent long-range electrochemical process. The perfect stoichiometry of the electrochemical defluorination is well-documented,<sup>2</sup> but we cannot suggest any plausible explanation why amalgams are superior agents also for the primary "chemical" defluorination as compared to pure alkali metals (cf. refs 17 and 26).

The F1s spectrum of C–LiF (Table 1 and Figure 1b) indicates only the presence of LiF, but the C1s region shows a considerable amount of carbon other than elemental (C<sup>α</sup>, 284.6 eV) and CH<sub>x</sub> impurity (C<sup>β</sup>, 284.8 eV). The C1s spectrum is similar to that observed for C–LiF from ordinary PTFE.<sup>25</sup> We tentatively assign the characteristic, strong C<sup>δ</sup> peak to surface COOH groups, which are formed during a short contact (minutes) of the sample with air oxygen and humidity. This contact is unavoidable in our setup, since the preparation of C–LiF samples (manipulations with mercury) in situ is excluded technically. The larger intensity of the CH<sub>x</sub> peak in C–LiF (C<sup>β</sup>, see Table 1 and Figure 1 a, b) is understandable in terms of the increased surface area of the carbonized samples. The assignment of peaks C<sup>β</sup> and C<sup>γ</sup> to a defined surface oxygen group is not straightforward, because of the large variability of surface oxides on carbons.

The appearance of a resolved peak of surface oxides at 289 eV is unusual among carbon materials, which mostly exhibit several overlapping peaks at 285–289 eV. A single peak appears only for special materials, such as graphite oxide containing solely C–O–C and C–OH moieties (287 eV).<sup>28</sup> The sensitivity of C–LiF against surface oxidation apparently corresponds to the presence of the reactive sp<sup>2</sup>-hybridized structure of the carbon skeleton (cf. eq 1a).<sup>2</sup> Although we would theoretically expect a relation between the C hybridization state and the binding energy of C1s,<sup>29</sup> a deeper discussion of the C<sup>α</sup> peak in C–MF is not possible because of the sample decomposition.

**3.2. Atomic Force Microscopy.** AFM imaging at lower magnification (scanned area 1 μm<sup>2</sup>) shows the heterogeneous character of the PTFE film on a silicon wafer (Figure 2). Similar images were obtained also on other supporting materials. The regular corrugation of the PTFE film varied within the range of about 10–50 nm. The uncovered areas were detected by the atomic force modulation technique, which distinguishes between surfaces of different hardness. High-resolution images could only be obtained on selected areas with the lowest corrugation.

The AFM (lateral-force) image (Figure 3) of the chosen homogeneous region of the PTFE film deposited on the Si wafer shows individual PTFE molecules. A well-resolved molecular structure exhibits all PTFE chains oriented parallel to the direction of deposition. Figure

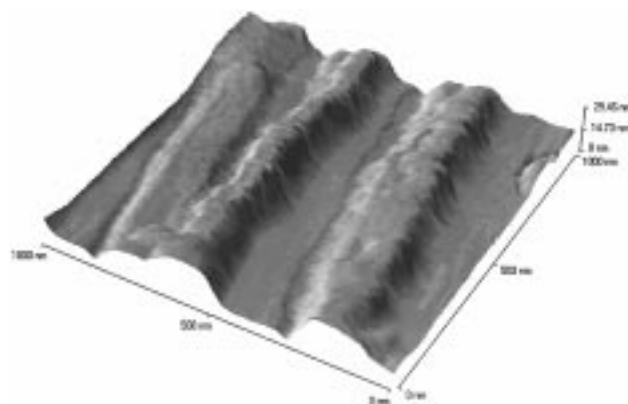


**Figure 2.** Low-resolution AFM image of oriented PTFE film deposited on silicon wafer by a hot-dragging technique. Scanned area: 1 × 1 μm.

3b displays an AFM lateral-force image with scanned area of 6.6 × 6.6 nm<sup>2</sup> filtered by 1-Dimensional fast Fourier transform (1D FFT,  $k = 0.8 \text{ nm}^{-1}$ ). It shows a lateral periodic modulation, which could be ascribed to the helical conformation of the fluorine atoms.<sup>13,30</sup> The expected periodicity of the AFM image along the chain (0.84 nm for 13<sub>7</sub> helix<sup>13</sup>) is roughly demonstrated in our AFM pattern, although the actual identity periods depend considerably on the conditions of the FFT used. Consequently, we cannot distinguish between the two possible conformations of the PTFE molecule: 13<sub>6</sub> helix (stable below 19 °C) and 15<sub>7</sub> helix (stable between 19 and 30 °C).<sup>31</sup>

AFM patterns of the carbonized film (C–LiF) are shown in Figures 4–7. At low magnification, the morphology of C–LiF (Figures 4 and 6) resembles that of the starting PTFE film (Figure 2). Separated vertical ribs of the height of several tens of nanometers correspond to the original features of the virgin PTFE. This conclusion matches the SEM data obtained by Dousek et al.,<sup>32</sup> who have studied a PTFE foil cut from a polymer block on a lathe. The micron-sized relief at the PTFE surface (introduced by imperfections of the cutting edge of the lathe knife) was reproduced also on the carbonization product, C–LiF. (It even survived subsequent heating at 950 °C in He, when LiF melted out; cf. Fig. 4 in ref 32).

Spherical grains observed for the C–LiF surface (Figure 4) seem to indicate a nucleation-type of reaction. This is expected for PTFE with microscopically nonuniform surface reactivity. In this case, the reaction starts from single separated points and spreads spherically until it reaches the boundary of neighboring reaction center, where it stops. The observed spherical grains consisted of a relatively hard material, which is not affected by scanning of the cantilever tip in the contact mode. The spherical grains seem to demonstrate that the volume of PTFE increases as a result of "Li insertion". (On the macroscopic scale, the thickness of the C–LiF film was found to be larger by a factor of 1.22 as compared to that of PTFE<sup>7</sup>).

To visualize better the morphological changes caused by carbonization, we have prepared two-phase films containing both PTFE and C–LiF areas on the same

(28) Papirer, E.; Guyon, E.; Perol, N. *Carbon* **1978**, *16*, 133.

(29) Jackson, S. T.; Nuzzo, R. G. *Appl. Surf. Sci.* **1995**, *90*, 195.

(30) Bunn, C. W.; Howels, E. R. *Nature* **1954**, *174*, 549.

(31) Clark, E. S.; Muus, L. T. *Z. Kristallogr.* **1962**, *117*, 119.

(32) Dousek, F. P.; Jansta, J.; Baldrian, J. *Carbon* **1980**, *18*, 13.

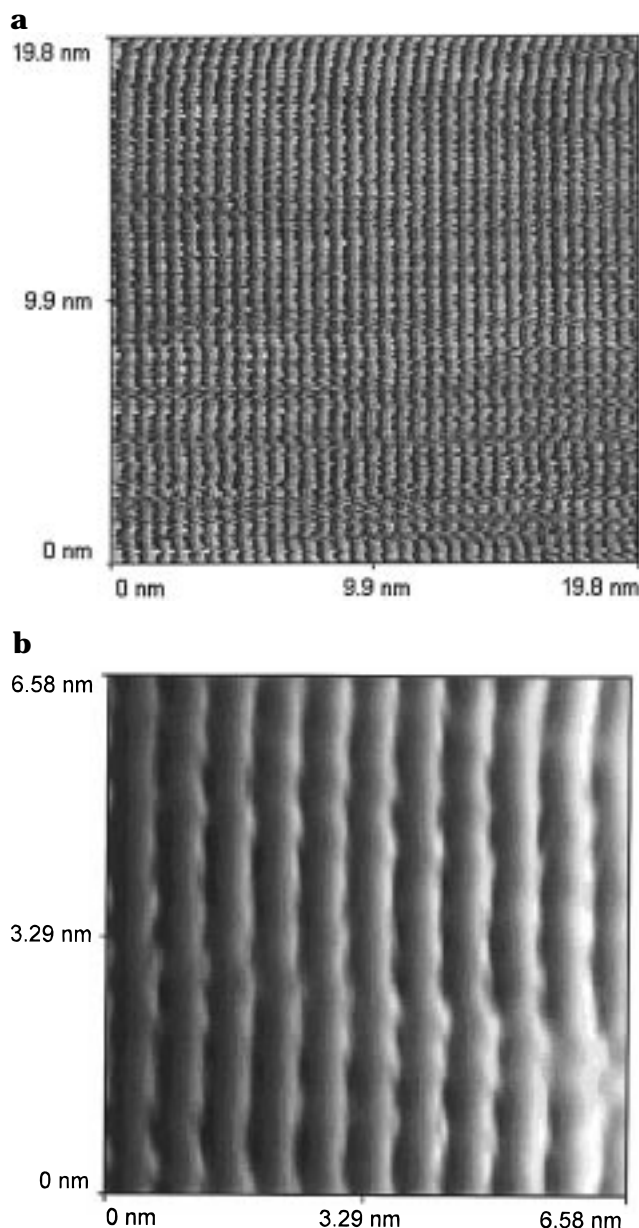


**Figure 3.** AFM image of PTFE molecules in highly ordered PTFE film deposited on a Si wafer. Scanned area  $20 \times 20$  nm (a) and  $6.6 \times 6.6$  nm (b). Panel b was obtained after 1D FFT filtration.

support. The sample was prepared by immersing the Si/PTFE sheet into the Li amalgam, while care was taken that only part of the film was dipped into the amalgam and the remaining part was intact. Good samples showed a sharp reaction zone at the interface between the carbonized and virgin PTFE (C–LiF/PTFE interface, Figures 5 and 6). The AFM material-analysis performed by modulated force (hardness analysis) confirmed that the material composition of the two areas is different (Figure 5). The reaction zone is clearly visible also on the AFM topographic images, where the carbonized area exhibits enhanced corrugation as compared to the relatively smooth PTFE surface (Figure 6).

The defluorination of ordinary PTFE with Li amalgam yields cubic LiF nanocrystals with an average size of 3.3 nm (from the Scherrer's X-ray line broadening).<sup>2</sup> However, the composition and morphology presumably changes upon contact with air, when the carbon surface

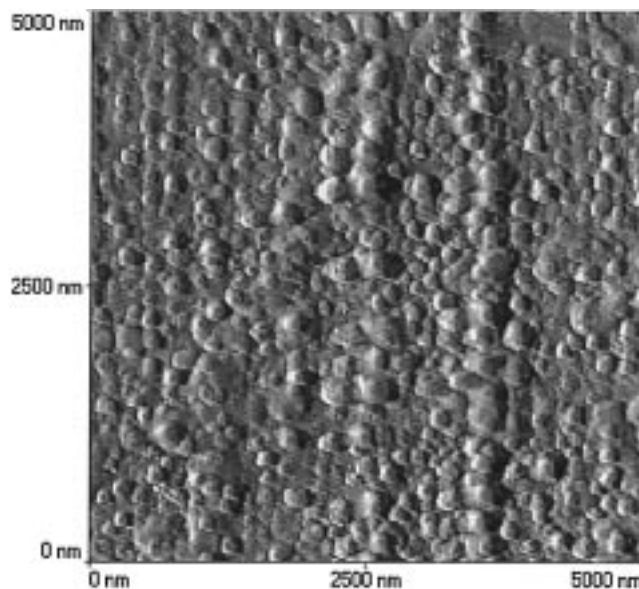


**Figure 4.** AFM image of PTFE film deposited on a Si wafer after reductive defluorination with Li amalgam, with a scanned area of  $5 \times 5 \mu\text{m}$ . Vertical ribs are dragging patterns which survived the defluorination process (cf. Figure 2).

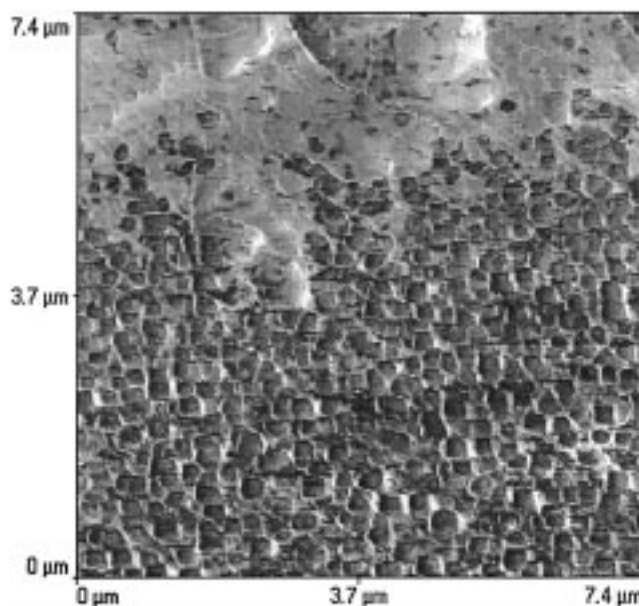


**Figure 5.** AFM force modulation material (hardness) analysis of the reaction zone formed on partly carbonized PTFE film: (top, light color) intact PTFE, (bottom, dark color) C–LiF composite formed by reaction with Li amalgam.

is oxidized (cf. XPS results, section 3.1). It is known that LiF tends to recrystallize into larger crystals when C–LiF is in contact with air or other reactive environment, while both the LiF recrystallization and chemical modification of carbon synergically accelerate each other.<sup>2</sup> Cubic objects of ca. 300 nm size are visible in Figure 5, but they cannot be safely identified as LiF. A high-magnification AFM image of the carbon film shows only an amorphous surface without any sign of oriented structure (Figure 7). The originally ordered PTFE film (Figure 3) is fully reconstructed after reductive defluorination and loses the periodicity visible at the molecular level. However, this is very probably a secondary effect introduced by the air-induced degradation of the sample (cf. XPS results, section 3.1). Unfortunately, our

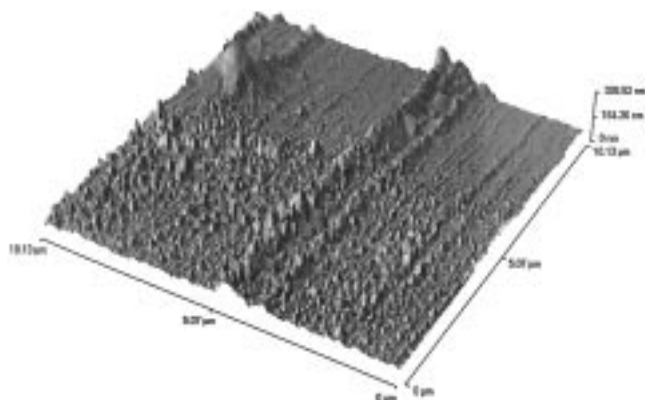


**Figure 6.** AFM topographic image of the reaction zone formed on partly carbonized PTFE (cf. Figure 5): (top right) intact PTFE film, (bottom left) C–LiF composite.

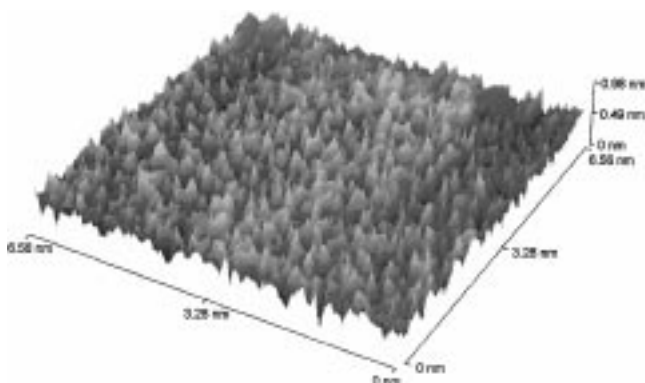


**Figure 7.** Molecular resolution AFM image of defluorinated highly ordered PTFE film (C–LiF). No sign of the formerly ordered structure (cf. Figure 3) can be observed.

AFM instrument does not allow microscopic studies to be carried out in inert atmosphere.

**3.3. Raman Scattering.** The above-mentioned problem of air degradation of C–MF (cf. sections 3.1 and 3.2) is avoided with in situ Raman spectroscopy, where both the sample preparation and spectroscopic measurements can easily be carried out in a high vacuum (see Experimental Section). Figures 8 and 9 (curves B) show the Raman spectra of C–LiF and C–NaF films, respectively. In both cases, the spectra B are rather noisy because the Raman scattering of the thin film is weak. For comparison, we show in Figures 8 and 9 (curves A) the Raman spectra of C–LiF and C–NaF layers (thickness about 1  $\mu\text{m}$ ) made on ordinary PTFE foil. In this case, the Raman signal is stronger (less noisy) because the sample layer thickness is larger by 1–2 orders of magnitude.

All spectra show a characteristic line at about 2000  $\text{cm}^{-1}$  which corresponds to a stretching vibration of  $\text{sp}^2$  carbon chain.<sup>4,5</sup> This stretching mode is arbitrarily assigned to polyyn, although there are no strong arguments for this particular isomer of  $\text{sp}$  carbon chain (cf. eq 1a and discussion thereof).<sup>2</sup>

The spectra display a second line at lower frequencies, which can be deconvoluted into two components, around 1200–1300 and 1400–1500  $\text{cm}^{-1}$ , respectively. This doublet (called also D and G lines) occurs also in ordinary C–MF materials (as in curves A; cf. ref 4). It is characteristic for polycrystalline graphite-like carbon with  $\text{sp}^2$  bonds. The graphite-like (graphene) structures

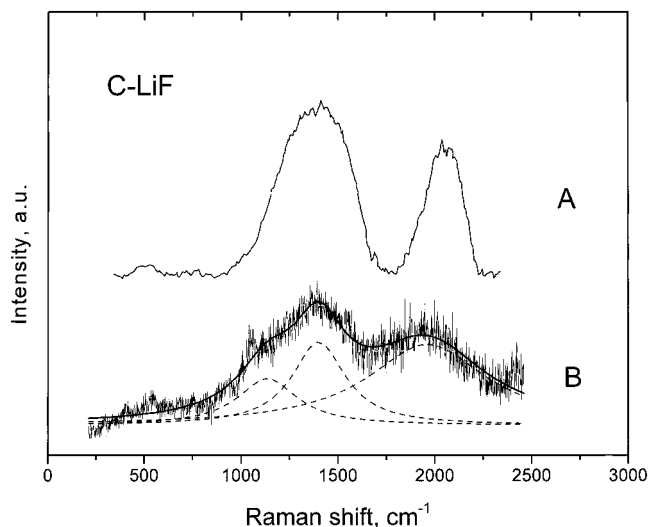


**Figure 8.** Raman spectrum of the C–LiF layer made from PTFE by the action of Li amalgam: (A) C–LiF from ordinary PTFE foil, (B) C–LiF from highly oriented PTFE film deposited on glass. (The intensity scale in AU is not common for the spectra A and B.)

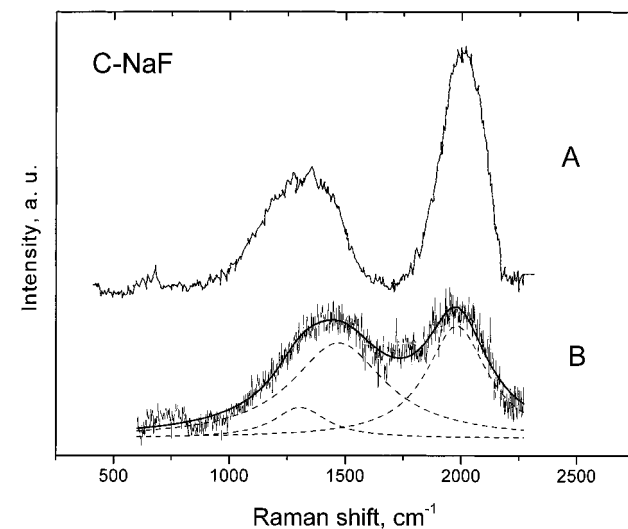
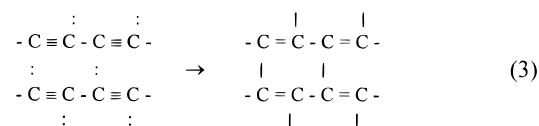


**Figure 9.** Raman spectrum of the C–NaF layer made from PTFE by the action of the Na amalgam: (A) C–NaF from ordinary PTFE foil, (B) C–NaF from highly oriented PTFE film deposited on glass. (The intensity scale in AU is not common for the spectra A and B.)

are formed via cross-linking of polyyn:



The relative intensity of the  $\text{sp}^2$  doublet ( $I_G/I_D$ ) correlates with the in-plane graphite crystallite size,  $L_a$ :<sup>33</sup>

$$L_a = 4.4I_G/I_D \text{ [in nm]} \quad (4)$$

The found  $L_a$  values for oriented C–MF films are around 10 nm (cf. Figures 8 and 9 and eq 4), i.e., they are significantly larger than the  $L_a$  values for ordinary

C–MF estimated from Raman spectroscopy<sup>4</sup> or X-ray diffraction<sup>34</sup> (in the latter case,  $L_a$  values of 0.6–1.6 nm were reported for carbon from C–LiF, which is below the Raman-detectable limit<sup>4</sup>). This analysis shows qualitatively that the cross-linking (eq 3) is more pronounced for an array of parallel chains in highly oriented C–MF films as compared to ordinary C–MF materials. A statistical mixture of unoriented polyynes contains less sp carbon atoms within the bonding distance from a neighboring polyyne chain; i.e., the formation of graphene (eq 3) is obstructed. Hence, the cluster of unordered polyynes in C–MF is sterically better stabilized against cross-linking.

The polyyne line for oriented C–NaF (curve B, Figure 9) shows relatively lower intensity as compared to that of nonoriented C–NaF (curve A, Figure 9). This seems to confirm a higher cross-linking rate (higher graphene/polyyne ratio; cf. previous paragraph) for oriented films. However, any comparison of Raman intensities must be considered with care because of the unknown contribution of resonance enhancement. We should note that the UV–vis absorbance maximum of C–MF depends on the layer thickness.<sup>4,27</sup> Consequently, the smaller intensity of the polyyne line in oriented C–MF does not necessarily mean the smaller concentration of polyyne, but solely the smaller resonance enhancement in thin films.

The frequency of the polyyne peak is lower for highly oriented C–MF films ( $M = \text{Li}, \text{Na}$ ) as compared to the nonoriented C–MF (Figures 8 and 9). This indicates larger conjugation lengths for oriented films.<sup>4</sup> The conjugation length is larger for C–NaF compared to C–LiF, both for oriented and nonoriented C–MF. This reflects a better spatial separation of polyyne chains in C–NaF, caused by the presence of the more bulky NaF component.<sup>2,4,5</sup> Nevertheless, the product's structure is still far from an "infinite" polyyne, which is expected for a defect-free defluorination of a PTFE macromolecule (eq 1a). (The infinite polyyne should theoretically exhibit a Raman band around  $1800 \text{ cm}^{-1}$ .)<sup>4</sup> The smallest fitted experimental frequency equals  $1974 \text{ cm}^{-1}$  (for oriented C–NaF; Figure 9, curve B), which translates into about 18 carbon atoms in an unperturbed sp conjugation.<sup>4</sup> This result compares favorably with conjugation lengths for various other electrochemical carbons.<sup>2,5</sup>

A rigorous discussion of conjugation lengths should consider that the cited model<sup>4</sup> is valid only for an

electroneutral polyyne, whereas carbons from fluoropolymers are always n-doped (cf. eq 1b).<sup>2,7</sup> The doping can modify the force constants (Raman frequencies) of polyyne (as in the case of other conducting polymers), but there is no relevant theoretical model for polyyne available in the literature. On the other hand, the doping levels for C–LiF, C–NaF, and C–KF (from ordinary PTFE) are almost independent of the alkali metal type.<sup>2</sup> Consequently, the qualitative trends in conjugation lengths of C–MF may still be correct, even if we neglect the doping.

#### 4. Conclusions

The defluorination with Li and Na amalgams was studied, for the first time, on a highly ordered PTFE film made by friction deposition. XPS and Raman spectra indicate a full conversion of PTFE into a composite of carbon and alkali metal fluoride, C–MF. This evidences that the amalgam reduction is superior as compared to the reduction with pure alkali metals, where a complicated mixture of products has been reported. The carbonized film is sensitive to surface oxidation in air, which is reflected by a characteristic C1s spectrum.

Significant structural changes on both the macroscopic and molecular levels were observed by AFM in the film after defluorination. Only the macroscopic (micrometer scale) surface relief of PTFE was reproduced also in C–MF. Experiments failed, up to now, to demonstrate in C–MF also the highly ordered molecular structure of the precursor. This is probably due to the sample degradation during AFM measurement in air.

Raman spectroscopy evidences a partial formation of sp-bonded carbon chains in C–MF. The conjugation length is higher for oriented C–MF as compared to nonoriented C–MF and for C–NaF as compared to C–LiF. Oriented C–NaF shows (in terms of the conjugation length model) about 18 carbon atoms in an unperturbed sp chain.

**Acknowledgment.** This work was supported by the Grant Agency of the Czech Republic (contract no. 203/98/1168) and by the Grant Agency of the Academy of Sciences of the Czech Republic (contract no. A4040605). Thanks are due to Dr. Z. Bastl (J. Heyrovský Institute, Prague) for XPS analyses and to Dr. L. Dunsch and M. Krause (IFW Dresden) for their assistance with Raman measurements.

CM9807438

(34) Cervinka, L.; Dousek, F. P.; Jansta, J. *Philos. Mag. B* **1985**, *51*, 603.